NAL PROPOSAL No. 26

Correspondent: K. Wendell Chen
Department of Physics
Princeton University
P. O. Box 708
Princeton, New Jersey 0854

FTS/Off-net: 609-599-3511
452-4400

HIGH MOMENTUM TRANSFER INELASTIC MUON SCATTERING AND TEST OF SCALE INVARIANCE AT NAL

K. W. Chen
Princeton University

L. N. Hand
Cornell University

June, 1970

HIGH MOMENTUM TRANSFER INELASTIC MUON SCATTERING AND TEST OF SCALE INVARIANCE AT NAL

K. W. Chen

Princeton University

L. N. Hand

Cornell University

ABSTRACT

We propose a relatively simple first stage experiment with muons in the 50-150 GeV range. The experiment is designed to optimize conditions for testing scale invariance while providing some information about the final state, as a test of various theories of high energy interactions.

The proposed use of an iron spectrometer and of a high Z (> 1) target with a low intensity ($\sim 10^6$/sec) muon beam should greatly reduce the cost and complexity of the experiment and especially ease the construction of the beam. It may even be possible to make an adequate muon beam for this purpose from the planned 3.5 mrad high intensity pion beam. A higher intensity muon beam can be used to extend the range in q^2.

Information gained in this first experiment could greatly assist the planning of a more sophisticated experiment proposed for the high intensity μ beam.

I. Introduction

A. Physics

For a variety of reasons, inelastic muon scattering may be an even more interesting and effective way to probe nucleon structure at NAL energies (50-150 GeV and above) than in the past. Although the muon remains a mystery and should be studied in its own right for some clue as to the dynamics of the muon-electron difference, at NAL we encounter, for the first time, more muons than electrons. Previously the virtual photon has served us well as a useful way to insert a controllable amount of energy and momentum into a proton or neutron - the muon beams under discussion have adequate intensity to continue these studies. Although the level of sophistication in muon experiments has not in the past been perhaps as high as that encountered in the electron-scattering experiments, we feel that this situation is not intrinsic to the use of muons and will yield to a sustained effort to obtain high quality information. Muons will be useful because one observes directly an interaction "vertex" as a function of the dynamical variables. The usefulness of having such a probe, which is also the case for the inelastic neutrino experiments is immediately apparent when one considers the highly specific predictions for this process by parton models, for example, and the sum rules for integrals of W_2 and W_1. Although the form of the theories may change, we believe firmly that experiments with muons will present some of the strongest challenges to future dynamical theories due to the relative simplicity of a single interaction vertex. The comparison with the corresponding neutrino experiments will be necessary for separating vector and axial vector terms in the latter reactions.

Of course this simplification may be only apparent, since virtual photons, at least at small q^2, may behave in many respects like hadrons, through dif-

fraction dissociation. One immediate question to be answered concerns whether there exists a qualitative change in the nature of virtual photon interaction in the deep inelastic limit or whether some extension of the basic vector dominance idea can be maintained. Specifically, then, the following arguments can be presented for an early look at muon inelastic scattering:

The scale invariance predicted by Bjorken[1] and discovered by the SLAC inelastic electron scattering experiment[2] may or may not hold as one proceeds to even higher momentum transfers and energy losses. (See Figure 1) Of course if we have reached a truly asymptotic region without encountering "substructure", it will hold. In neutrino reactions, if the W meson exists, scale invariance is violated by the finite spatial extent of the interaction region caused by the W propagator. An analogous statement would appear in the muon scattering if the apparent (from the SLAC results) granularity of the proton charge distribution were not caused by fundamental entities like partons or quarks[3] but just by the "lumpiness" of the charge distribution predicted in the field theory from the cloud of virtual (non-exotic) hadrons around the proton. In more technical terms, one would like to know the limit of νW_2 as $X \to 0$ $(X = \frac{q^2}{2M\nu})$ and whether scale invariance holds as q^2 becomes very large.

To go beyond the observations of the muon alone, one would like to know if scale invariance holds in the individual reaction channels, and what the multiplicity and transverse momentum distributions look like as functions of q^2 and ν. As a special case of this, the hypothesis of "limiting fragmentation" discussed by Yang, Benecke and others[4] predicts a separate fragmentation of the target nucleon and, by diffraction dissociation, the virtual photon. These fragments, in the high energy limit, approach a limiting probability distribution in the appropriate rest frame. It is predicted that the

average multiplicity associated with the target nucleon will be the same, regardless of whether the nucleon is excited by pp, πp, or μp collisions. Even crude measurements on the final state can test these theories and whether scale invariance holds for partial cross sections.

B. General Discussion of Experimental Approach

We believe that rather simple experimental apparatus will yield 10% answers quickly and cheaply, permitting efficient design of an "omnibus" detector at a later stage. We do not believe that it will be necessary to sacrifice the quality of the information of most immediate interest.

The specific ideas proposed here are:

1. The use of an iron spectrometer to achieve 7% resolution at 100 GeV very cheaply and simply. The experience of one of us (K. W. C.) in building a cosmic ray spectrometer has proved valuable and has given us confidence that such a spectrometer will meet specifications.
2. The choice of geometry and reaction kinematics to simplify and render more direct the test of scale invariance at these energies. As is discussed below, such a test can be related to observables in a way that minimizes systematic effects and permits increased precision.
3. The use of a low intensity muon beam (10^6/sec) eliminates the need for extensive collimation and momentum selection. An intense pion beam 1-2% of which decays into muons can easily produce such a beam and this experiment could possibly serve, for example, as the beam stop for the 3.5 muon high intensity beam. About 100 meters of drift space plus an 8-10 meter Be plug and an 18D72 bending magnet will be required to form the muon beam. (See Figure 2) This low

intensity can be used without achieving unacceptably low rates by using an interaction target of 100 gm/cm^2 spaced out over a distance which varies from 1-2 meters in the course of the experiment. Use of a high Z target requires some understanding of the A dependence of the cross section. An A dependence which differs from $A^{1.0}$, and experimentally equals $A^{0.91\pm.02}$ at 18 GeV and below, is predicted for $q^2 = 0$ by the "shadowing" model of Ross and Stodolsky[5]. Agreement with Margolis' calculations using this model is seen in the total γA cross section measurements done at SLAC[6]. The same model predicts a q^2 dependence shown in Figure 4, which reveals the region over which some shadowing might appear. Of course, by changing targets we can test the prediction of this model that $\sigma \sim A^1$ for the q^2 and ν values of interest here. An extension of this proposal to lower q^2 values would allow observation of the predicted shadowing but we prefer to concentrate first on the highest values of q^2 and ν available.

At even higher intensities ($10^7 \sim 10^8$ μ/sec), we give up the possibility of observation of the reaction products, but can obtain improved statistics on the region $q^2 > 100$ (GeV/c)^2. Availability of the intense beam at an early stage would dictate use of this apparatus to look at ultra high q^2 as soon as the beam becomes available.

4. The last new feature of this experiment will be the use of a reaction target distributed through the body of a 1-2 meter spark chamber with 40 5-cm gaps. If lead is used as the target material then we have about 16 radiation lengths available and over most of the chamber have a very high conversion probability for gamma rays. The combina-

tion of wide gaps and poorly conducting plates will support a large number of tracks and we hope to make significant observations on the multiplicities of charged and neutral tracks, and obtain information about π^{o} transverse momentum distributions from the angular distribution of the observed gamma rays. If the average multiplicity is ~ 6 with 60 GeV energy loss, the average momentum is 10 GeV/c and the particles tend to emerge within a 40 mrad cone. Typically at 1 meter from the vertex, 6 tracks or developing showers are contained inside about a 3" diameter circle.

Ten X and Y Charpak chambers with 100% efficiency for multiple tracks will be inserted in the body of the production chamber. By combining this with the wide-gap optical chamber information we will obtain the multiplicity of fast charged particles, the angular distribution of these about the momentum transfer direction and from the observed gamma ray showers data concerning the π^{o}'s.

We now turn to a more detailed discussion of these points.

II. Concept of Experimental Test of Scaling

Consider the effect on $\frac{d^2\sigma}{d\Omega dE}$ for inelastic muon (or electron) scattering of the transformation

$$E \to \lambda E$$

$$E' \to \lambda E'$$

$$\sin\frac{\theta'}{2} = \frac{1}{\sqrt{\lambda}} \sin\frac{\theta}{2}$$

$$q^{2'} = \lambda q^2$$

$$\nu' = \lambda\nu$$

$$X' = X = \frac{Q^2}{2M\nu}$$

If we ignore the very small change in $\cos^2\frac{\theta}{2}$ at small or even moderately large angles (essentially all angles of interest at these energies), then we find that $X = Q^2/_{2M\nu}$ (with W_1) remains invarient and, provided νW_2 is scale invarient, We have then

$$\frac{d^2\sigma}{d\Omega dE'} \to \frac{1}{\lambda}\frac{d^2\sigma}{d\Omega dE'} = \frac{1}{\lambda}\left(\frac{\alpha}{2E_o \sin^2\frac{\theta}{2}}\right)^2\left[W_2 \cos^2\frac{\theta}{2} + 2W_1 \sin^2\frac{\theta}{2}\right] \qquad (1)$$

Note that the proportionality to $1/\lambda$ is independent of the value of $R = \sigma_L/\sigma_T$.

Furthermore, $\Delta\Omega\Delta E'$ is invarient under this transformation so the counting rate decreases as $\frac{1}{\lambda}$, even if there is a spread in the incident beam energy, providing the relative distribution of energies remains the same.

Upon further investigation, we find that it is possible to extend this transformation so that most of the experimental effects such as finite resolution in determining the scattered muon momentum and angle do not affect the inter-comparison of different energies, i.e. different values of λ.

This means that we can compare experimental distributions directly and

ascertain immediately any violations of scale invariance.

Figure 3 shows this concept of testing scale invariance. The figure indicates the dependence on λ of the various experimental variables. If we scale the apparatus for each energy point (say 50, 100, 150 GeV) we remove the effects of:

1. Measurement error on the incident muon direction.
2. Beam divergence from multiple scattering in the Be filter.
3. A spread (from the pion decay spectrum) in the incident muon energies.
4. Multiple scattering in the target chamber and in the iron plate spectrometer.
5. Effects of dE/dx in the spectrometer.

Table I shows the actual statistics which might be obtained using an extrapolation of the SLAC results per 100 hours running time at 10^6 100 GeV muons per second. The number of events at 50 and 150 GeV is the same provided we make the appropriate transformation and scale invariance holds.

III. Experimental Arrangement

A. The Muon Beam

The boundary conditions imposed by the absence of a specially designed muon beam led us to consider the experimental factors in approaching the limit of zero cost--i.e. what can be done using a low intensity muon (10^6/sec) beam derived from the "existing" 3.5 mrad. pion beam in a minimal way. In order to achieve good rates for large Q^2 scattering we increase the target density by using a high Z target. The general experimental arrangement, intended to replace the 3.5 mrad beam stop, is shown in Figure 2 and Figure 3.

B. Use of a High Z Target.

Use of the lower beam intensity ($10^6 \mu$/sec) and high Z target has a number of advantages and some obvious disadvantages. We start with the advantages:

1. At these intensities we may determine the muon energy directly by observing the incident muon before and after a deflecting magnet.
2. The reaction itself may be observed by combining the target material and a beam spark chamber. Much useful information can be obtained even without magnetic analysis of the reaction products. This can be simultaneous with the single arm experiment.
3. Problems with beam halo and monitoring are substantially reduced.
4. The high probability of γ-ray conversion might allow part of the radiative corrections to be checked experimentally.

The chief disadvantages of the dense high Z target are:

-1. One does not a priori know the A dependence of the scattering cross section, although one believes it is A^1 at large q^2.

-2. A very dense target will have a background from energetic knockon electrons which might tend to obscure the event through secondary showers. We have assumed 100 gm/cm^2 for this limitation, based on simple calculations of the probability of obtaining an energetic knockon and observations at 12 GeV pion interactions in an iron plate spark chamber with several hundred gm/cm^2.

For point -1 above, extensive calculations have been performed using the Stodolsky optical model (which is in agreement with the measurement A dependence of the total photon cross section for k from 2-18 GeV as determined by DESY and (SLAC). To the extent one sees a deviation from $\sigma_{\gamma A} = A\sigma_{\gamma N}$, one is observing

shadowing of the incident (virtual) photon. This surprising effect was explained by Stodolsky[5] and has been extensively studied by many authors including Gottfried and Yennie[7] and Brodsky and Pumplin[7]. The results (Figure 4) of an explicit calculation (using a cylindrical nucleus for ease in calculation) shows

1. This (μ scattering) experiment should not observe shadowing for $q^2 > 2$ i.e. over almost the whole kinematic region accessible at NAL $\sigma_A \sim A\sigma$.
2. If a measurement of σ_{TOT} for the muons is possible then these shadowing effects might be observed. The maximum effect is

$$\frac{\sigma_{\gamma A}}{A\ \sigma_{\gamma N}} = .43 \text{ for } k > 20 \text{ GeV}$$

$$Q^2 = 0 \text{ in Pb.}$$

Actual observation of the shadowing requires measurement of very small scattering angles and elimination of μ-e events. In this proposal we consider:

$$10 \text{ mrad} < \theta_\mu < 160 \text{ mrad}$$

This confines us mostly (but not entirely) to the deep inelastic region where the shadowing effects are expected to be less than a few present. This can be experimentally checked by using different targets.

C. Rate Calculation and Radiative Corrections

1. Cross Sections

Cross sections for muon scattering at these large momentum transfers and energy losses are of course unknown and can only be guessed. In order to provide some basis for planning the experiment we have taken an approximate fit to the SLAC electron scattering data, assuming that $R = \sigma_L/\sigma_T$ approaches a limiting value of 0.2 and that

$$\sigma_T\,(k,q^2) \cong \frac{\sigma_T(k,0)}{(1 + 2.6q^2 + q^4/k)} \qquad (2)$$

As was discussed in a recent Physical Review Letter by Nauenberg[8] the choice of this form guarantees the scale invariance of νW_2 in the limit $q^2 >> \nu^2$. In fact any functions of the form $1 + q^2\,f(q^2/k)$ in the denominator, plus the constancy assumed for $\sigma_T(k,0)$ guarantees a scale invariant $\nu\,W_2$. The above form only applies at some distance from the elastic limit $q^2 \to 2M\nu$.

Radiative corrections were applied to the cross sections, since these will be important in any precise test of scale invariance. It is found that these are not negligible, due to the appearance of the muon mass in the logarithm of the leading order terms.

Most, but not all of the radiative correction comes from the case where the muon radiates a photon in the forward direction and then scatters elastically at the lower energy. Both this, and the case where the radiation takes place after the scattering should be visible in the chamber and the extra photon might be identifiable by its collinearity with either the incident on scattered muon. However observation of this depends on the angular distribution and multiplicity of the reaction products, thus we prefer not to rely on it. The formulas used involve the

peaking approximation and were taken from Mo and Tsai[9].

As a typical example, figures 5 and 6 shows the calculated values of $\frac{d^2\sigma}{d\Omega dE'}$, for a variety of secondary muon energies E' at a fixed incident muon energy for 100 GeV. The rapid dependence on scattering angle ($\sim\frac{1}{\theta^4}$) and the slower dependence on E' are evident. Cross sections without radiative corrections are indicated by dotted lines and with radiative corrections by solid lines. It can be seen that in some cases the radiative correction is ~ 20-30%.

By looking at figures 5 and 6 we see that a precise muon experiment requires very good scattering angle resolution and at the same time requires very little in the way of resolution in E'; the 7% we hope to achieve being more than adequate for the experiment. This is a major reason why the simplicity of the iron spectrometer is well matched to this measurement.

2. Effect of Angular Error

A 1 mrad systematic error in θ at 10 mrad will make a 40% error in $\frac{d^2\sigma}{d\Omega dE'}$. At 60 mrad the same error is a 7% error in the cross section. Multiple scattering in the target chamber gives an rms $\delta\theta \sim 45$ mrad/$_{E'\ (Gev)}$. This is a random, not a systematic effect. The beam can be used to monitor systematic errors in θ. The importance of physically scaling the apparatus to eliminate systematic errors while checking scale invariance is clear. Of course thinner targets can be used for measurements at smaller values of θ, because the cross section is larger, but the measurement error in θ will always remain a problem for experiments which vary only the incident energy and not the geometry as well.

3. Counting Rate

Typical counts obtained and assumptions about the target and the beam in 100 hours of running are given in Table I. It should be emphasized that these are only best guesses, but plausible ones.

IV. Iron Spectrometer

A. General Consideration

In this section we describe in some detail the iron spectrometer we propose to use to analyze the inelastically scattered muons. Our prime motivation in considering the use of a toroidal solid iron magnet is that or tremendous reduction in power cost while permitting us to achieve a momentum and angular resolution sufficient for our purposes. The limiting factor of conventional spectrometers was that economics impose a limit on the magnitude of the magnetic field as well as the volume over which it acts. Cosmic ray spectrographs have been built using the solid iron magnet reaching a maximum detectable momentum in the neighborhood of 1000 GeV[10]. Our own experience with this concept has been also favorable.[11]

B. Magnet Parameters

We list in Table II the parameters considered in the spectrometer and Figure 7 shows a schematic diagram of one section of the iron magnet. The magnet is consisted of 4 identical sections each 1.5 meters long in the beam direction. Each section is in turn constructed from 120 low carbon magnet grade steel plates. The magnetizing coils each consisting of 500 turns of 10 s. w. g. lumax covered copper wire of total resistance $\sim 12\Omega$. At a current of ~ 20A a field of 18 Kg $\pm$ 0.7 Kg is expected.

C. Uniformity of Magnetic Field

It is important to know the variation of the uniformity of the magnetic field in both the wound and unwould areas. Fortunately previous experiences[10,11] give the actual search coil measurement of the field for both areas. Figure 8 shows the variation of field at locations 1, 2 and 3 for the wound area. The variation in field over a given plate is $\lesssim 1.6\%$ whereas the overall variation is of the order ± 2.5%. In addition a measurement of the leakage field from the iron surface reveals that it magnitude is of the order of 0.1% of the field within the iron. (Figure 9a).

With an expected uniformity of the order of 2.5% the momentum resolution of the muon spectrometer will not be limited by the uncertainty in the magnetic field but will be limited by the multiple scattering of muons in iron.

D. Momentum Resolution

If the magnetic field is sufficiently constant over the entire length, the accuracy to which the momentum of a muon can be determined is limited by the multiple scattering it suffers. Figure 10 shows the three alternatives available to determine the muon momentum:

1. Single measurement of incoming and exit angle. (Figure 10a). The fractional error of momentum determination varies as $L^{-1/2}$ since the magnetic deflection varies as L while the r.m.s. multiple scattering angle varies as $L^{1/2}$. Practical limitation in solid angle acceptance and minimum cut off energy optimizes the length L. In this case the momentum of the muon is given by

$$p = \frac{\chi K(1 + \epsilon^2/K^2)}{I(\theta_2) - I(\theta_1)} \qquad (3)$$

where θ_1 and θ_2 are incoming and exit angles,

ϵ = energy loss per unit length of iron,

$K = 300\ B$

χ = the lateral displacement of the emergent track position from the incident position, and

$I(\theta) = \exp.\ [\frac{\epsilon}{K}(\theta_1 - \theta)]\ (\cos\theta - \frac{\epsilon}{K}\sin\theta)$.

It is to be noted that at high energy (> 100 GeV) equation (3) reduces to the familiar form

$$p = \frac{KL}{\sin\theta_1 - \sin\theta_2} \tag{4}$$

The variation of the calculated incident momentum with the incident angle at 150 mrad is less than ± 2%. Figure 9b shows this variation. The resolution is limited by the ratio of the transverse momenta P_T^B (bending) and $P_T^{M.S.}$ (Multiple scattering)

$$\frac{\Delta p}{p} \sim \frac{P_T^{MS}}{P_T^B} \simeq \frac{0.286}{3.24}\frac{(GeV/c)}{(GeV/c)} \simeq 9\%$$

which is the greatest uncertainty. We show the photograph of the cosmic ray muon spectrometer now in operation at Princeton. (Figure 11).

2. Multiple measurements. (Figure 10b).

The previous analysis still applies. One would expect crudely the improvement on the momentum resolution goes as N where N is the independent number of measurements. The major disadvantage is that the solid angle factor decreases as L^2 and that no all measurements are wholly independent to exploit the $\sqrt{N}$ factor.

3. Multiple measurements of positions. (Figure 10c).

For a track of projected length L with transverse coordinates Y_n measured and longitudinal coordinates χ_n (n = 0,1,2,--N), the curvature and direction error are values of β and γ in the least square fit of

$$Y = \alpha + \beta\chi + \frac{1}{2}\gamma\chi^2 \qquad (5)$$

Variational techniques have been used to calculate the optimum resolution for a given magnet configuration from general considerations. The expected resolution is better in general than case 1). For 100 GeV muons, we found a momentum resolution of 7% for a measurement at four points by fitting the track to a circle. This is the approach that we have finally adapted in this proposal.

References

1. J. D. Bjorken, Physical Review 179, 1547 (1969).
2. E. D. Bloom et. al., Phys. Rev. Lett. 23, 930 (1969).
3. R. Feymann, International Conference on High Energy Collisions, Stony Brook, N. Y. (1969);
   S. D. Drell, Phys. Review, 187, 2159 (1969);
   H. Harari, Phys. Rev. Lett. 24, 286 (1970);
   J. D. Bjorken, E. A. Paschos, Phys. Rev. 185, 1975 (1969).
4. C. N. Yang, International Conference on High Energy Collisions, Stony Brook, N. Y. (1969).
5. L. Stodolsky, Phys. Rev. Lett. 18, 135 (1967).
6. D. O. Caldwell et. al., Phys. Rev. Lett. 23, 1256 (1969).
7. K. Gottfried and D. Yennie, Phys. Rev. 182, 1595 (1969);
   S. Brodsky and J. Pumplin, Phys. Rev. 182, 1795 (1969).
8. M. Nauenberg, Phys. Rev. Lett 24, 625 (1970).
9. L. W. Mo and Y. S. Tsai, Review of Modern Physics 41, 205 (1969).
10. R. M. Bull, W. F. Nash and B. C. Rastin, Il Nuovo Cimento 15, 349 (1965).
11. K. W. Chen et. al., R.S.I. to be published.

TABLE I

Total Counts in 100 Hours of Running

θ	Counts	$Q^2 = 2(100\ \text{GeV})(50\ \text{GeV})(1-\cos\theta)$
10-20 mrad	110,000	2.3 $(\text{GeV/c})^2$
20-40 mrad	20,000	9 $(\text{GeV/c})^2$
40-80 mrad	4,000	36 $(\text{GeV/c})^2$
80-150 mrad	200	$\approx$ 100 $(\text{GeV/c})^2$
Total	$\approx$ 134,000	

Assumed: 100 gm/cm^2 target

10^6 muons/sec.

$E' = 20\text{-}80$ GeV

$E_o = 100$ GeV

TABLE II

Torodial Magnet Spectrometer Specifications

Cross Section	1.5 m x 2 m
Total Length	6 m
No. of Sections	4
Length/Section	1.5 m
Energy Cut Off	10.74 GeV *
Material	1020 Steel
Lower Energy Cutoff (Straggling Limit)	20 GeV
$\oint B \cdot d\ell$	2000 Kg - in
No. of Turns/Section	5000
Total Coil Resistance/Section	12Ω
Magnetic Field in Iron	17.5 Kgauss.
Total Power Consumption	20 KW

* We use value of muon energy loss in iron

Figure Caption

1. Kinematic region for Muon inelastic scattering (q^2, ν plane) at NAL and SLAC.
2. A possible muon beam layout for μ inelastic scattering.
3. Plan view of proposed apparatus for test of scale invariance.
4. Predicted shadow correction versus $A^{1/3}$ for $\nu = 20$ GeV and for a cylindrical nucleus.
5. Variation of $\frac{d^2\sigma}{d\Omega dE'}$, with θ at a fixed E .
6. Variation of $\frac{d^2\sigma}{d\Omega dE'}$, with E' at a fixed θ.
7. Details of the iron magnet. Only one section is shown. Four sections are proposed for the spectrometer. a) Plan view. b) Schematic view.
8. Variation of magnetic field in the wound region as a function of the plate number. 3 positions shown in Figure 7a).
9. a) Leakage field versus distance away from the surface at position shown in (c).
10. Three alternatives for momentum determination with a iron spectrometer.
11. Photograph of a cosmic ray muon spectrometer at Princeton. Method of 10a) is used here.

KINEMATIC REGION
FOR MUON INELASTIC SCATTERING
(q^2, υ PLANE)

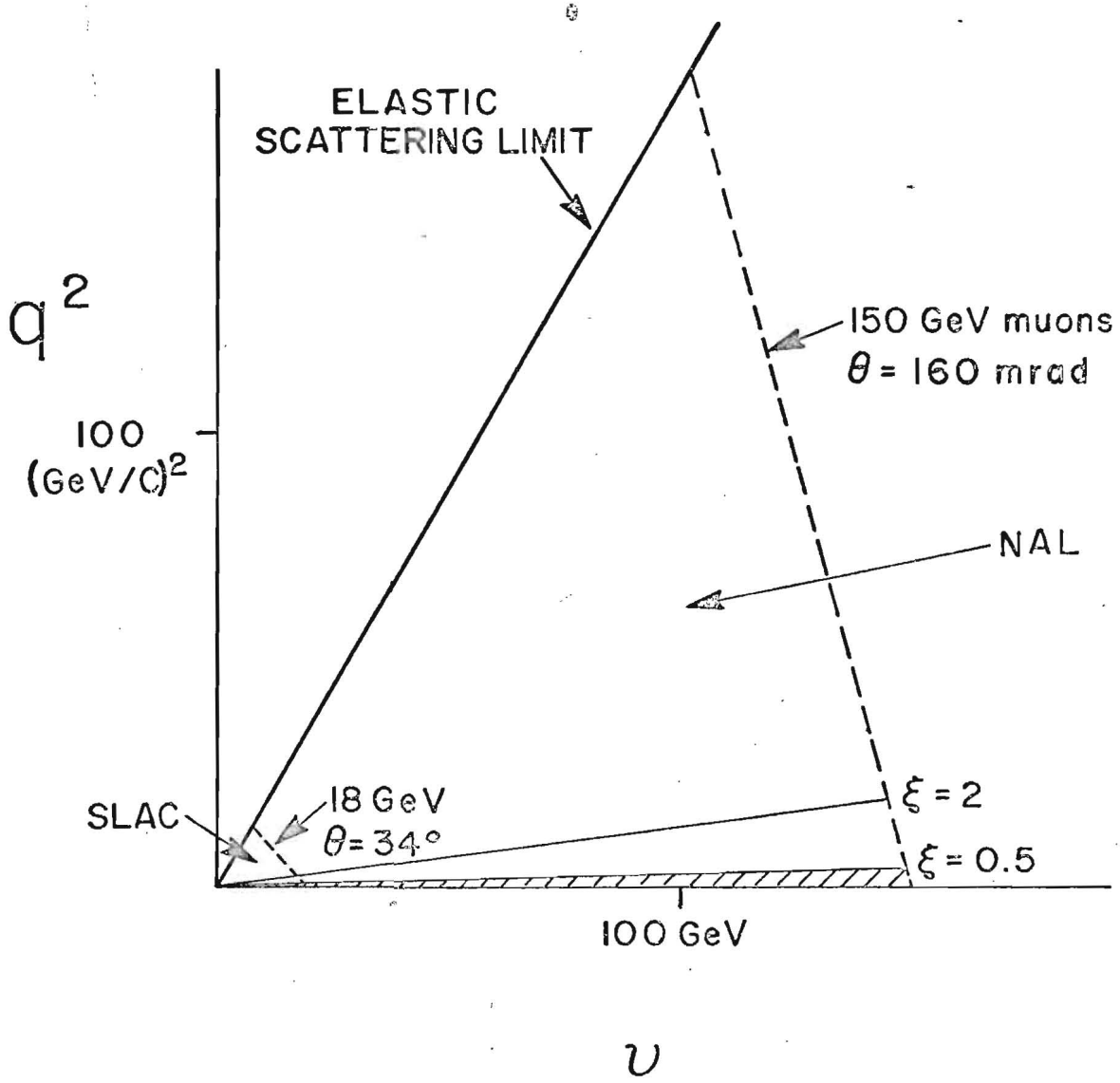

FIG. 1

A POSSIBLE MUON BEAM LAYOUT FOR μ INELASTIC SCATTERING

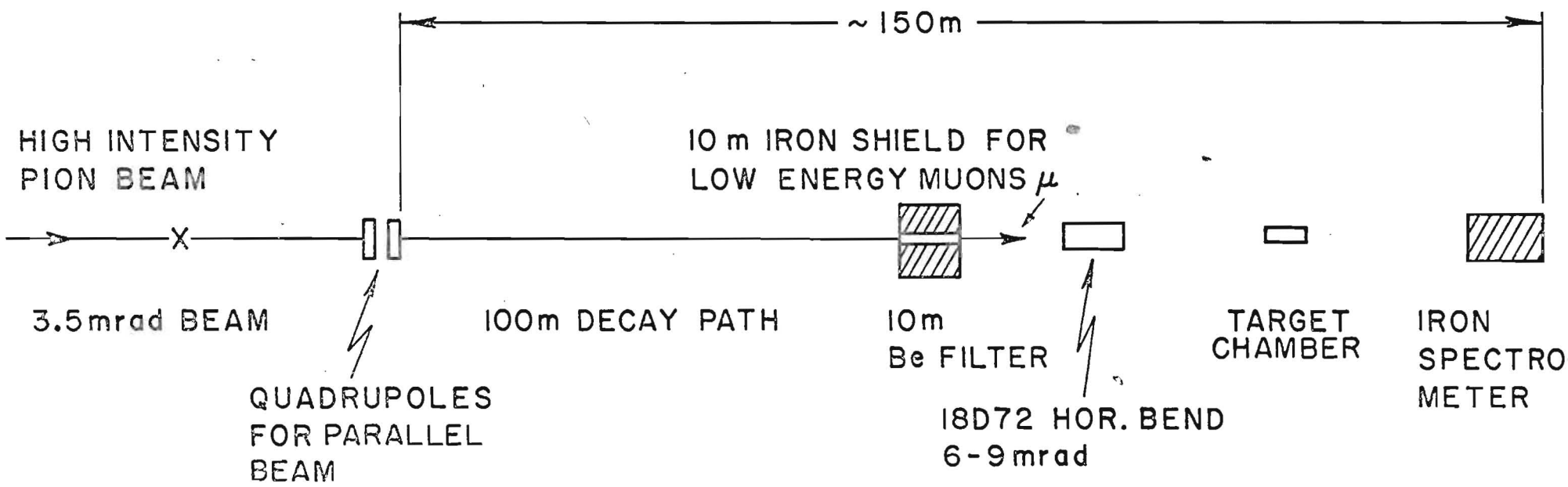

FIG. 2

PLAN VIEW OF PROPOSED APPARATUS FOR TEST OF SCALE INVARIANCE

[ALL TRANSVERSE DIMENSIONS REMAIN CONSTANT.]

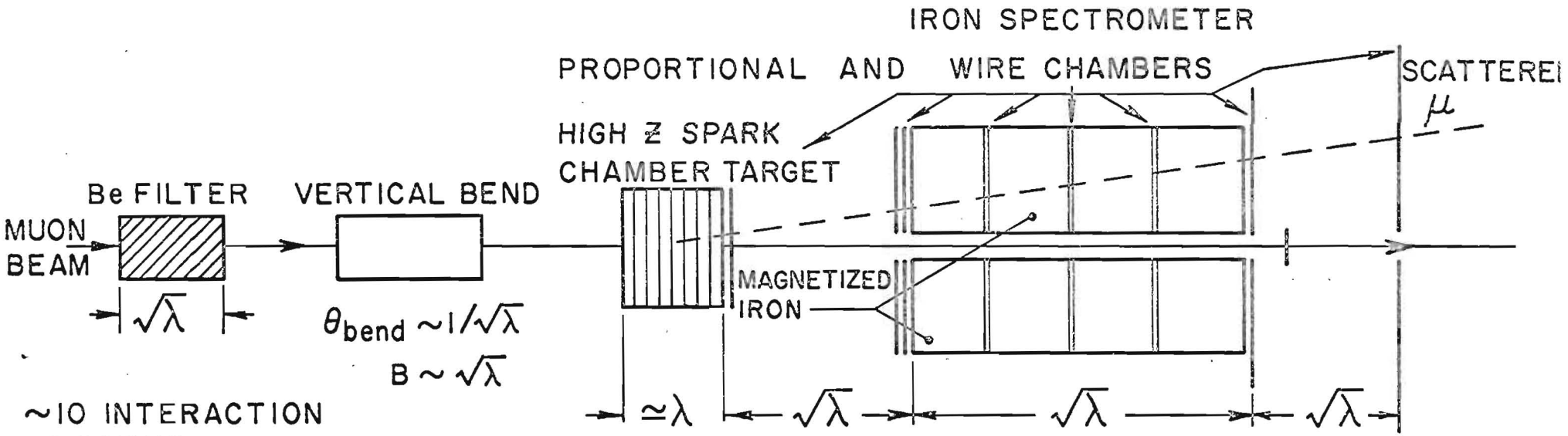

FIG. 3

PREDICTED SHADOW CORRECTION VS $A^{-1/3}$ FOR 20 GeV = ν
(CYLINDRICAL NUCLEUS)

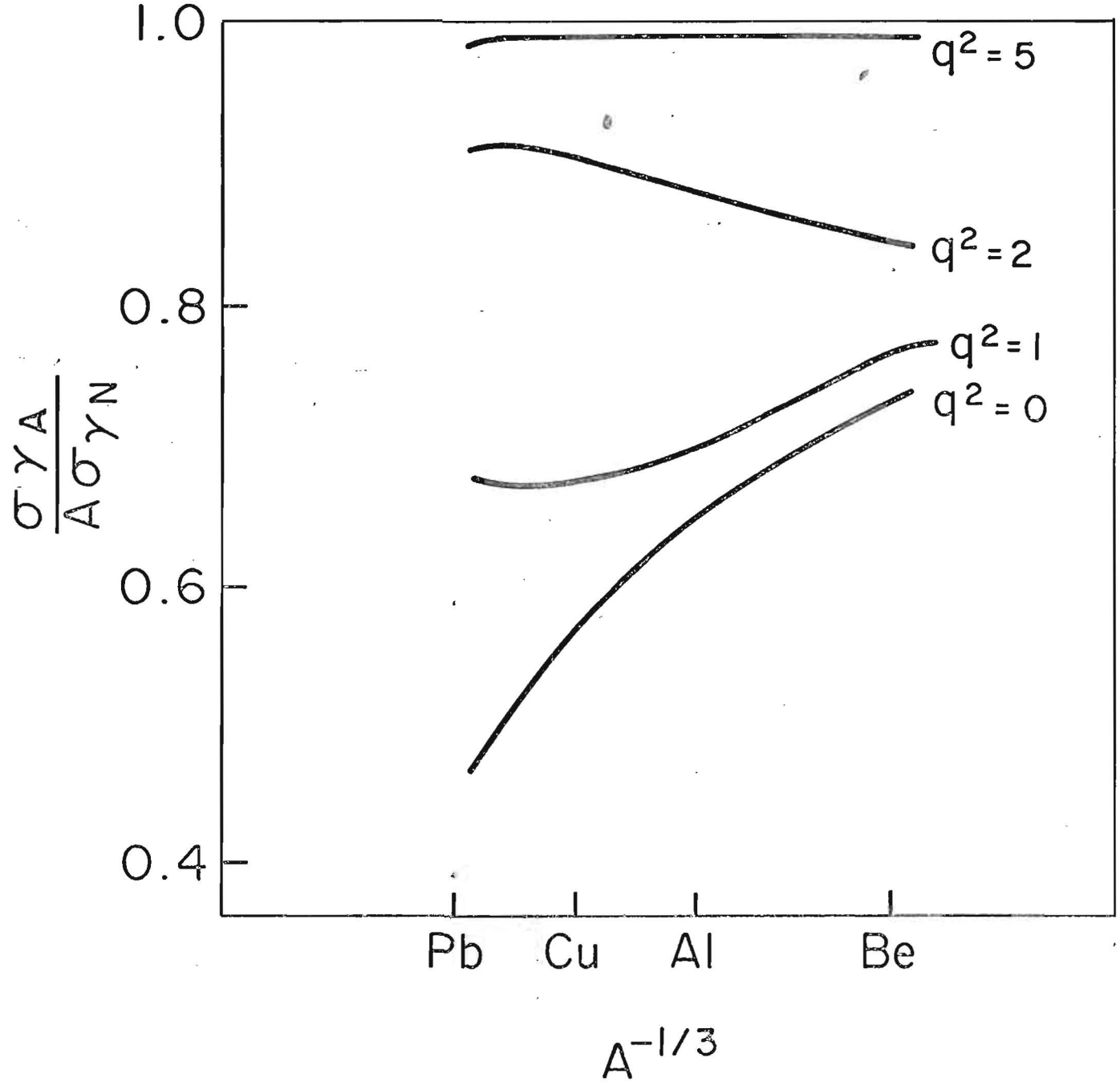

FIG. 4

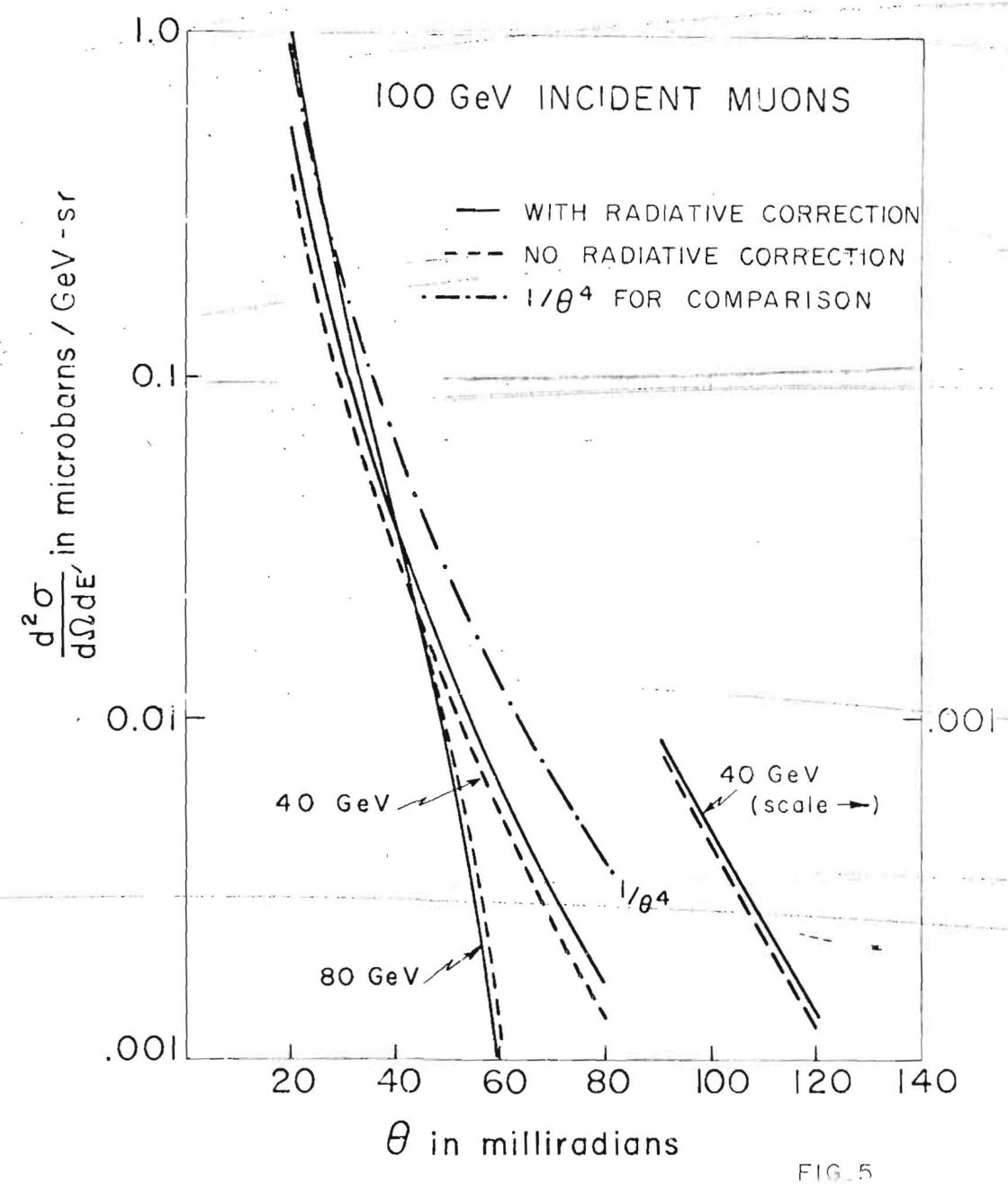
100 GeV INCIDENT MUONS
WITH RADIATIVE CORRECTION
NO RADIATIVE CORRECTION
1/θ⁴ FOR COMPARISON
1.0
0.1
0.01
.001
40 GeV
80 GeV
1/θ⁴
40 GeV
(scale →)
20
40
60
80
100
120
140
θ in milliradians
d²σ/dΩdE' in microbarns / GeV - sr

FIG. 5

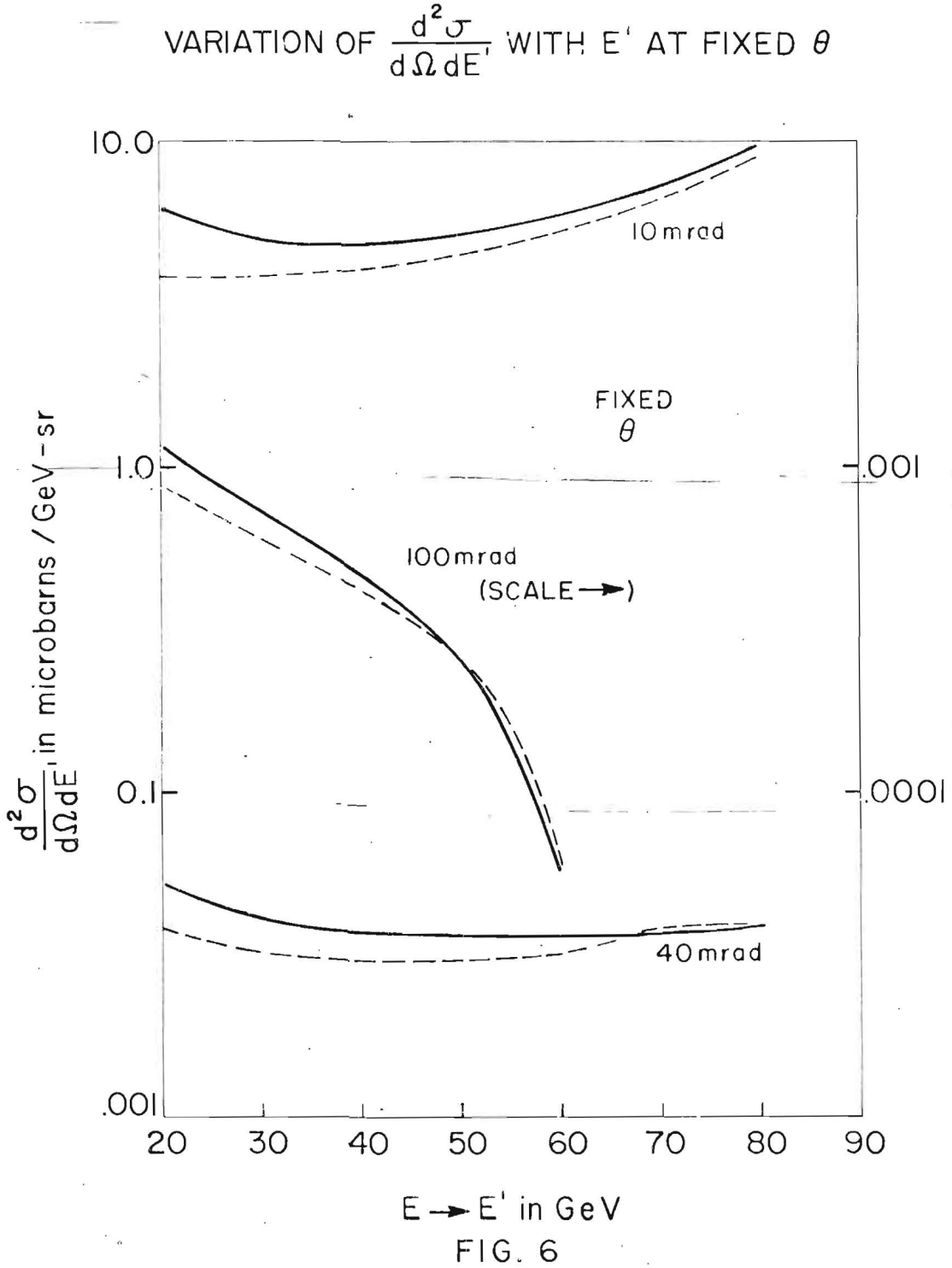
VARIATION OF $\frac{d^2\sigma}{d\Omega\, dE'}$ WITH E' AT FIXED θ
10.0
1.0
0.1
.001
.001
.0001
10 mrad
FIXED
θ
100 mrad
(SCALE →)
40 mrad
$\frac{d^2\sigma}{d\Omega\, dE'}$ in microbarns / GeV - sr
20
30
40
50
60
70
80
90
E → E' in GeV

FIG. 6

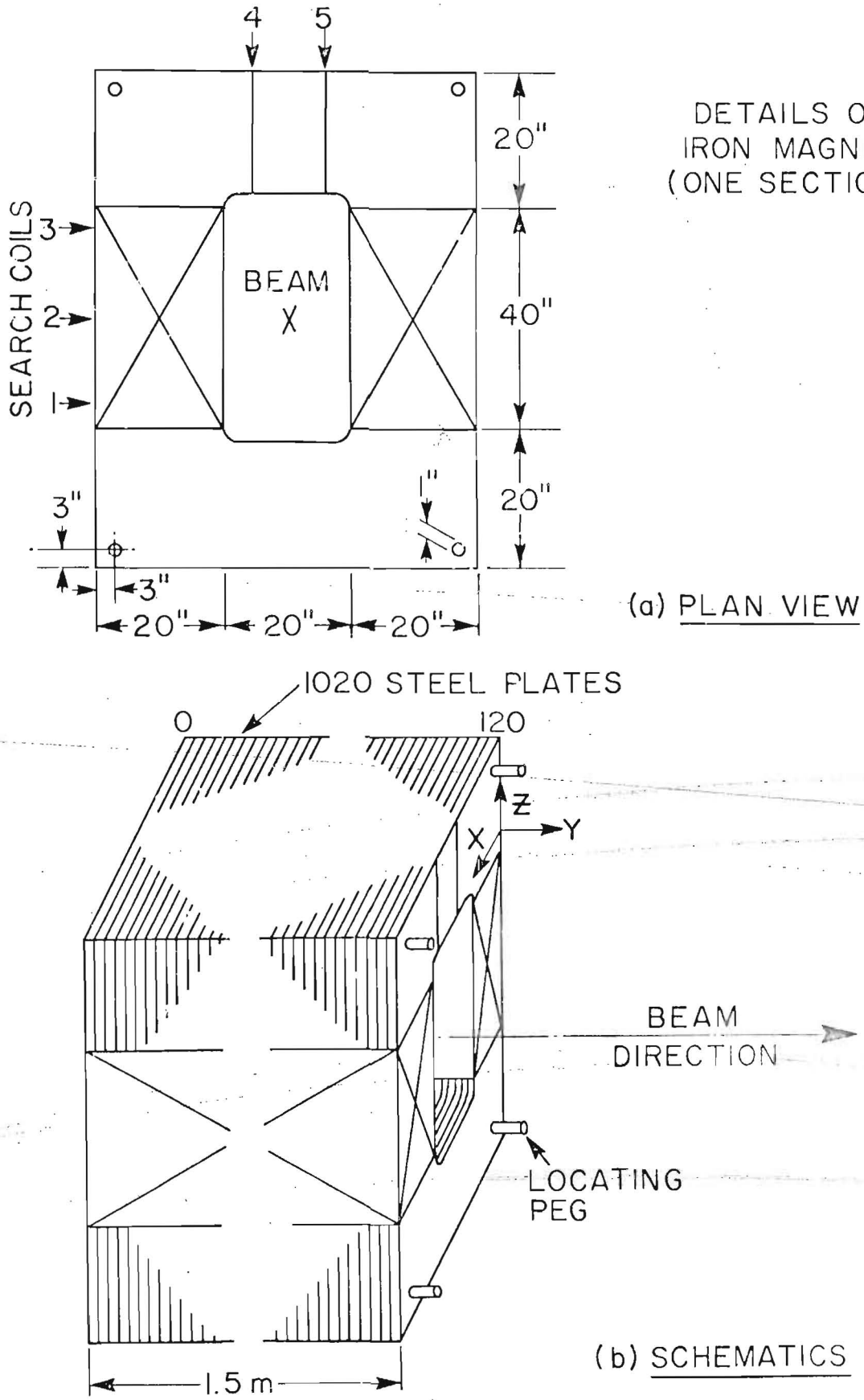

DETAILS OF
IRON MAGNET
(ONE SECTION)

FIG. 7

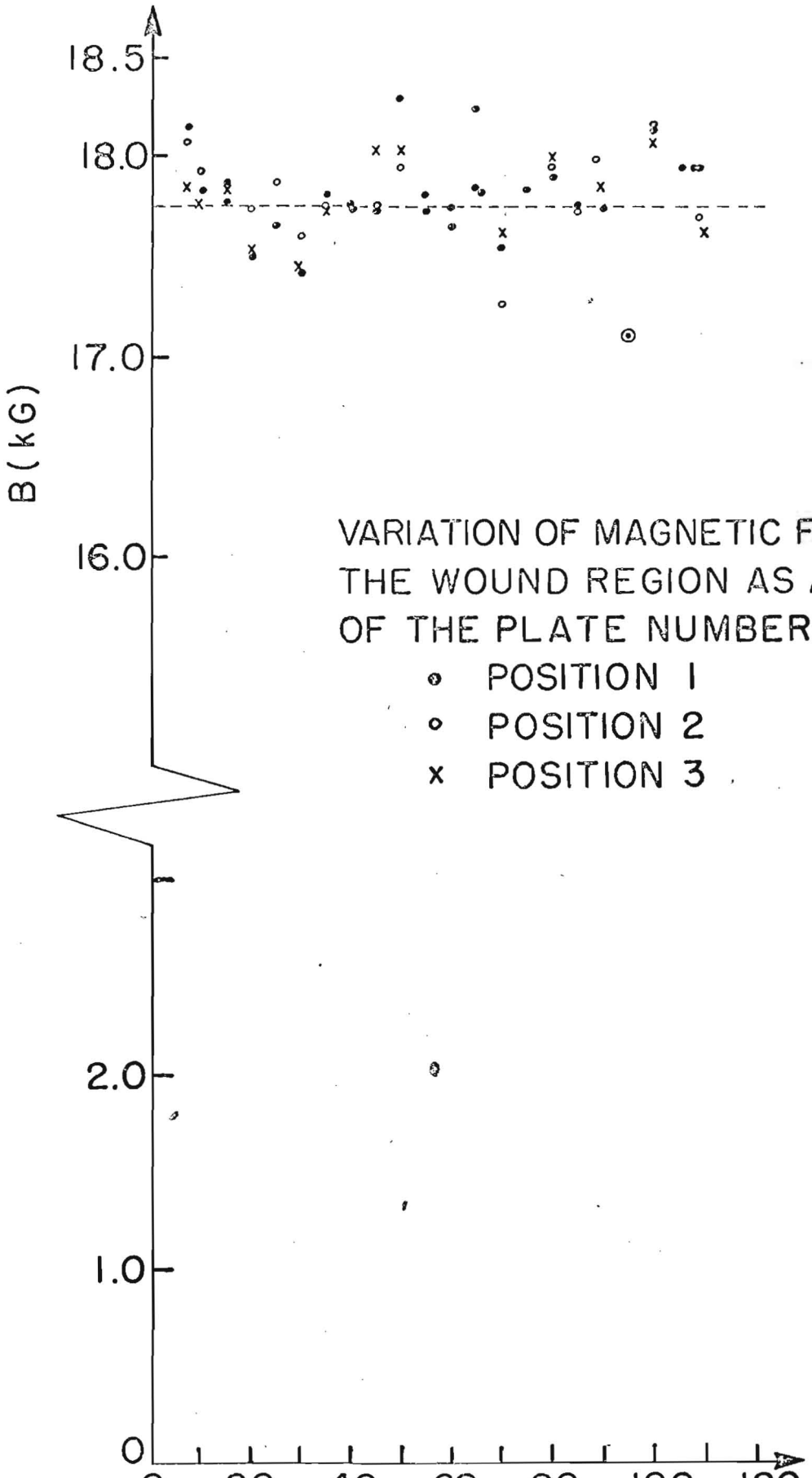

VARIATION OF MAGNETIC FIELD IN THE WOUND REGION AS A FUNCTION OF THE PLATE NUMBER.

- ⊙ POSITION 1
- ○ POSITION 2
- × POSITION 3

FIG.8

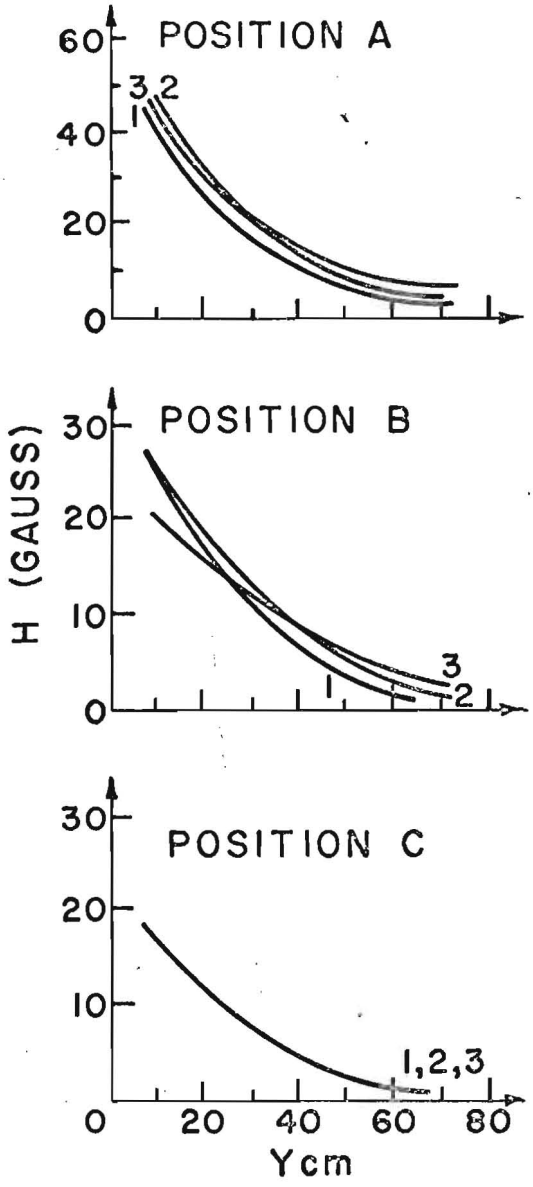

A) LEAKAGE FIELD AS FUNCTION OF DISTANCE FROM SURFACE AT POSITIONS SHOW IN (C)

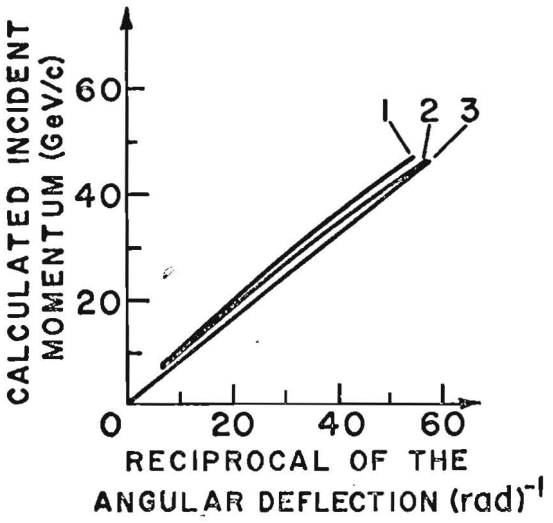

B) CALCULATED MOMENTUM vs $(\Delta \sin\theta)^{-1}$ AS FUNCTION OF INCIDENT AND EXIT ANGLES. (θ_1 = 160 mrad)

1 - $\theta_1 < \theta_2$

2 - $\theta_2 > \theta_1$

3 - AIR GAP

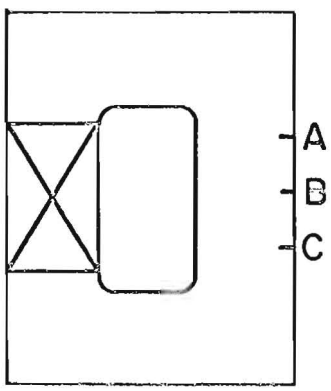

C) POSITION FOR MEASUREMENTS IN (C)

FIG. 9

3 ALTERNATIVE WAYS OF MEASURING MUON MOMENTUM

(a) SINGLE ANGLE MEASUREMENT

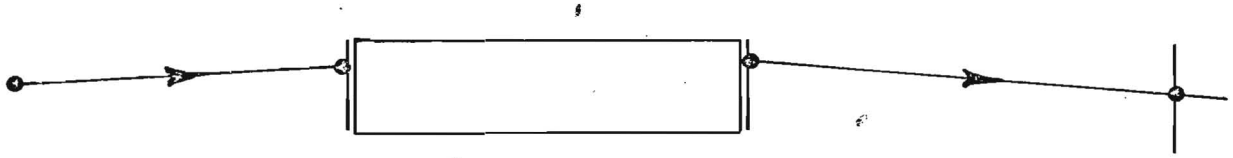

$$\frac{\Delta p}{p} \sim 10\%$$

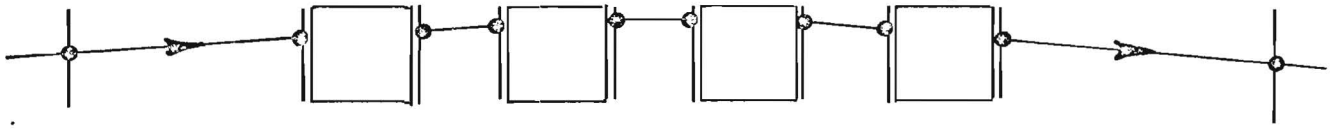

(b) MULTIPLE ANGLE MEASUREMENT

$$\frac{\Delta p}{p} \sim 8\%$$

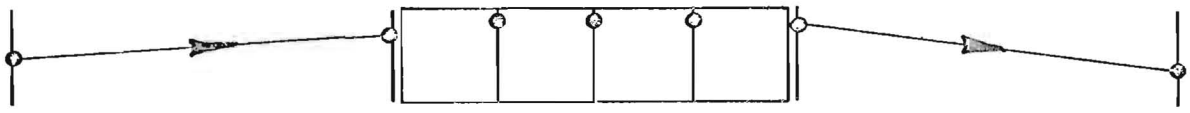

(c) MULTIPLE POSITION MEASUREMENT

$$\frac{\Delta p}{p} \sim 6.5\%$$

FIG. 10

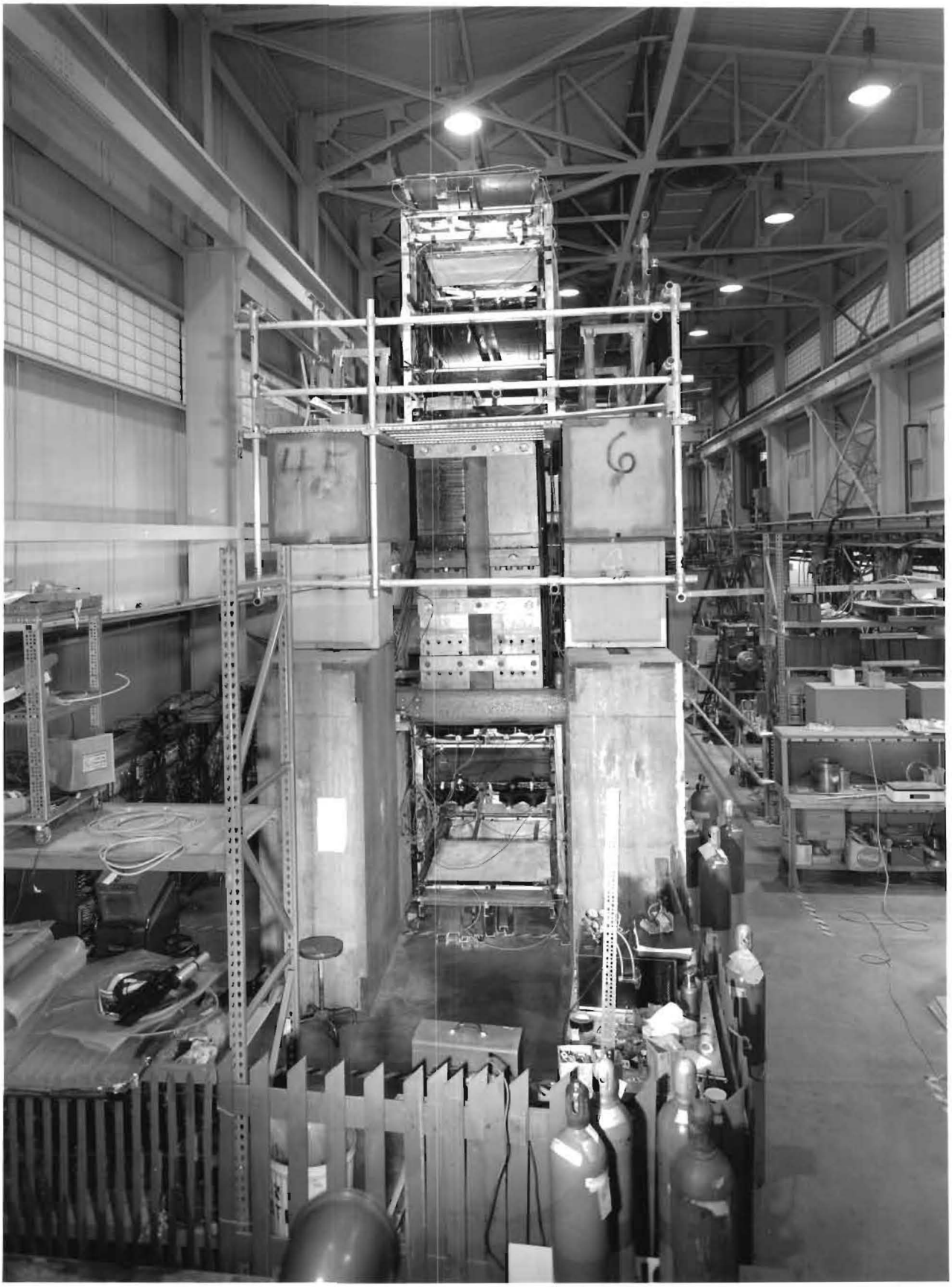

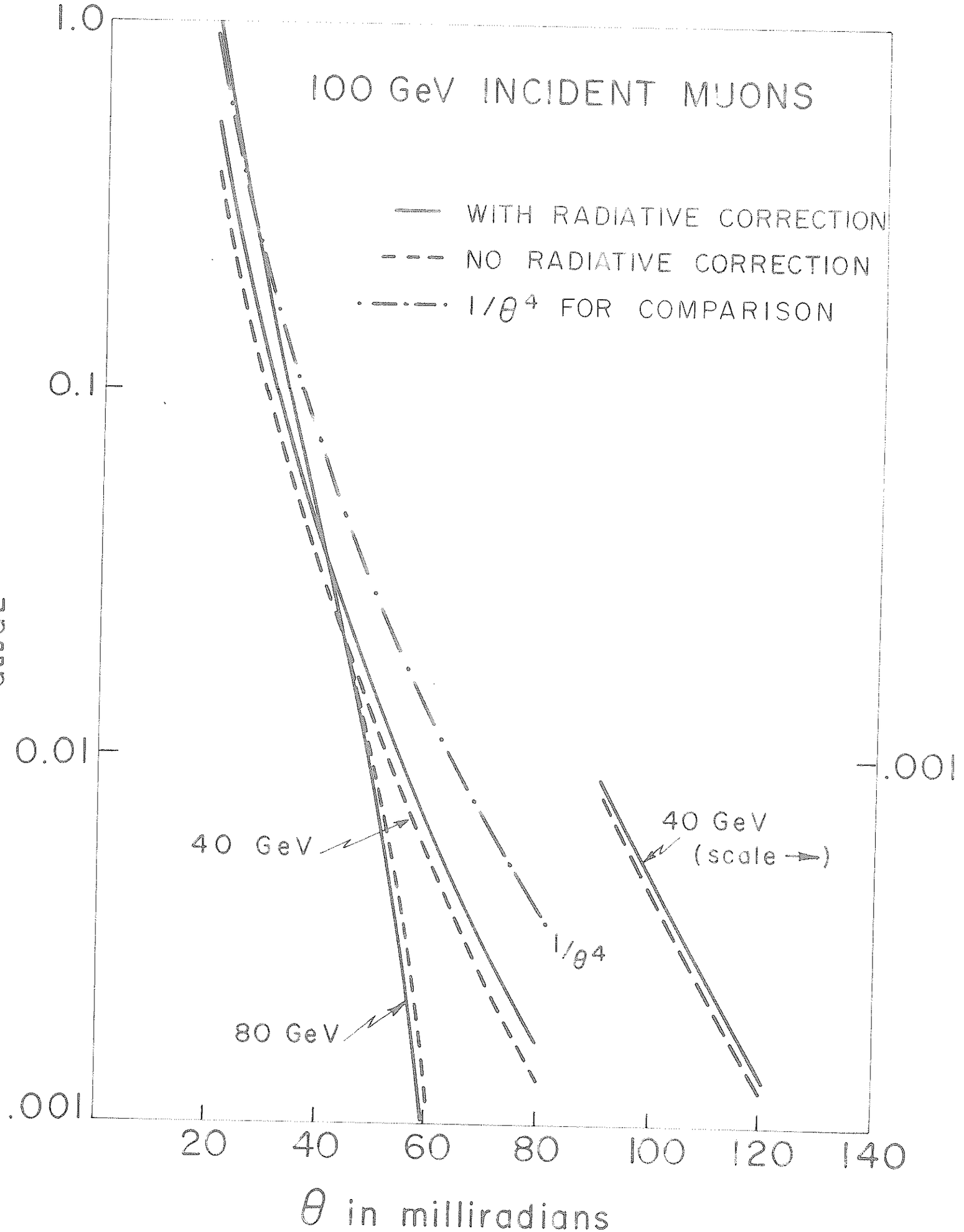
100 GeV INCIDENT MUONS
WITH RADIATIVE CORRECTION
NO RADIATIVE CORRECTION
1/θ⁴ FOR COMPARISON
1.0
0.1
0.01
.001
40 GeV
80 GeV
40 GeV (scale →)
1/θ⁴
20
40
60
80
100
120
140
θ in milliradians
d²σ/dΩdE' in microbarns / GeV - sr

FIG. 5

VARIATION OF $\frac{d^2\sigma}{d\Omega\, dE'}$ WITH E' AT FIXED θ

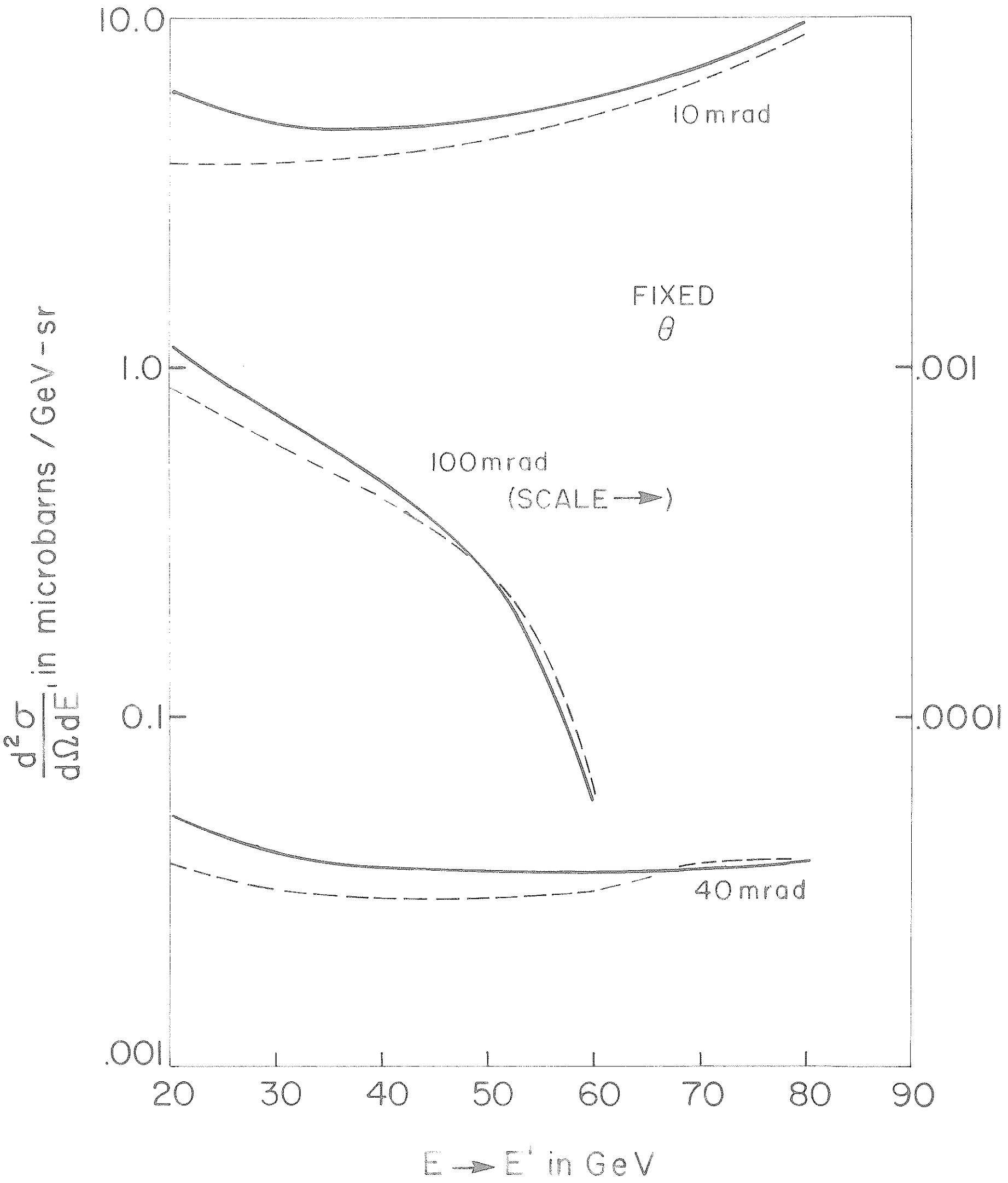

FIG. 6

DETAILS OF
IRON MAGNET
(ONE SECTION)

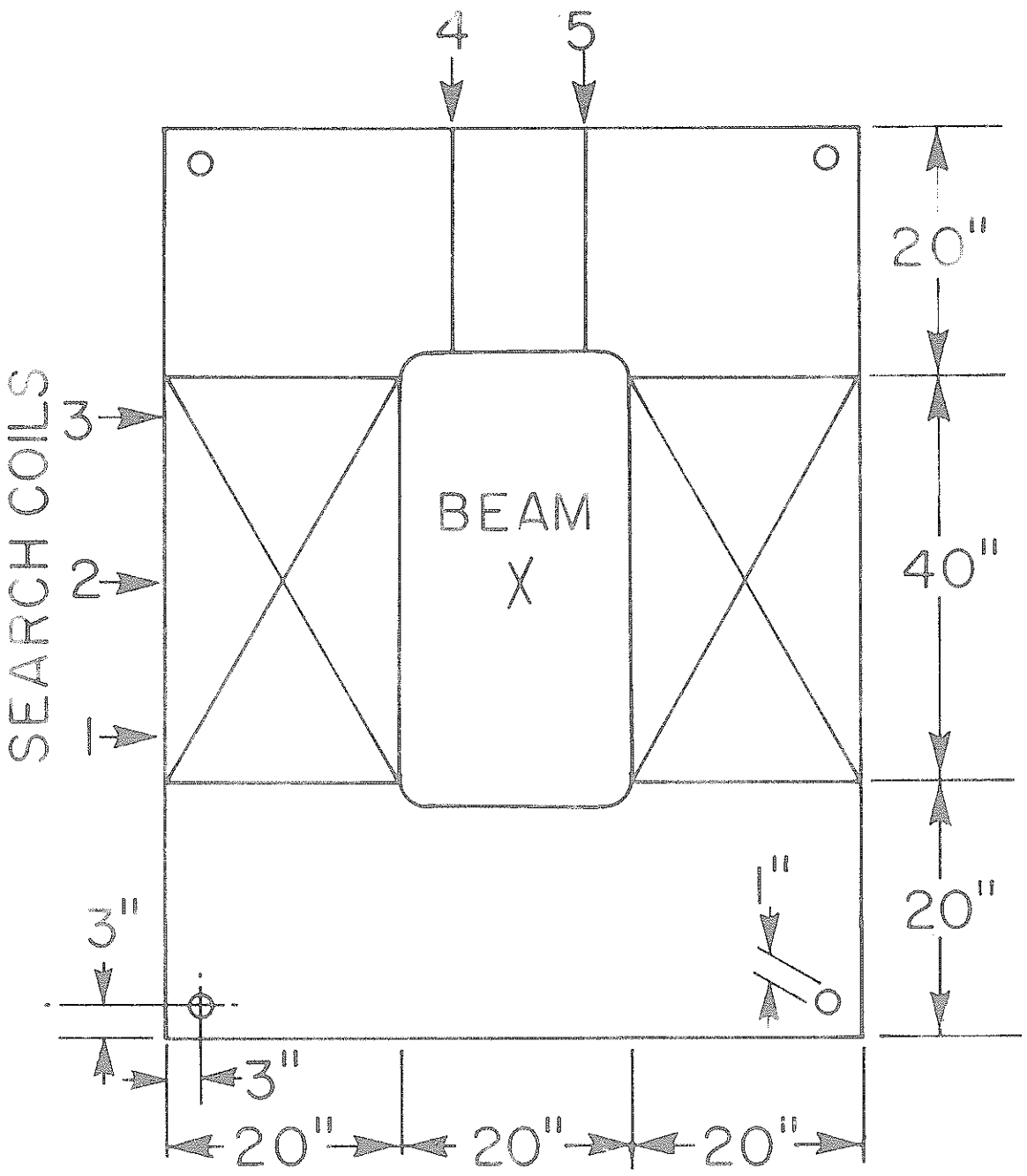

(a) PLAN VIEW

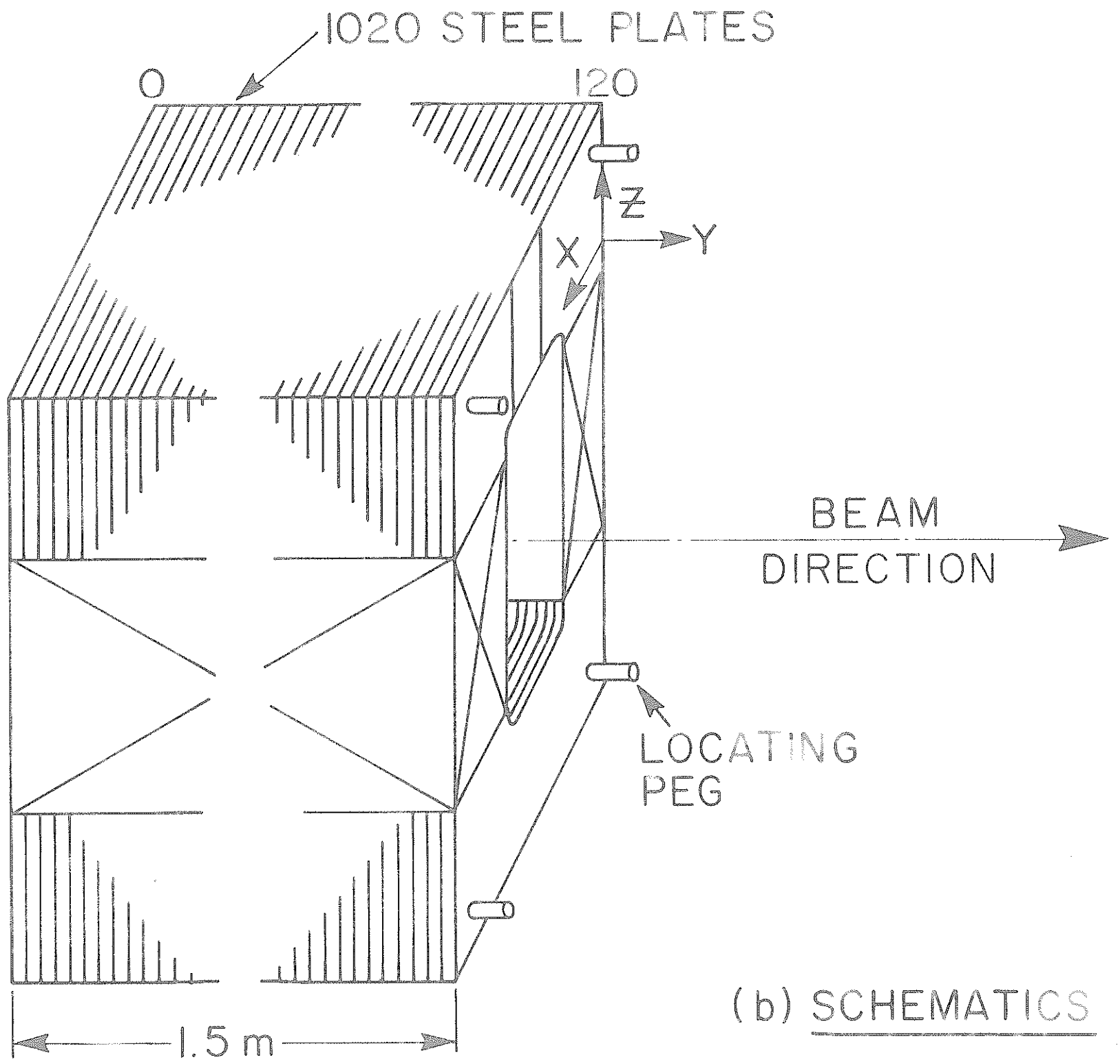

(b) SCHEMATICS

FIG. 7